Imperatoxin A Enhances Ca^{2+} Release in Developing Skeletal Muscle Containing Ryanodine Receptor Type 3

Thomas Nabhani,* Xinsheng Zhu,† Ilenia Simeoni,‡ Vincenzo Sorrentino,‡§ Héctor H. Valdivia,† and Jesús García*

*Department of Physiology and Biophysics, University of Illinois at Chicago College of Medicine, Chicago, Illinois 60607, USA, †Department of Physiology, University of Wisconsin at Madison, Madison, Wisconsin, USA, ‡Molecular Medicine Section, Department of Neuroscience, University of Siena, Siena, Italy, and §Dipartmento di Ricerca Biologica e Tecnologica, Istituto Scientifico San Raffaele, Milano, Italy

ABSTRACT Most adult mammalian skeletal muscles contain only one isoform of ryanodine receptor (RyR1), whereas neonatal muscles contain two isoforms (RyR1 and RyR3). Membrane depolarization fails to evoke calcium release in muscle cells lacking RyR1, demonstrating an essential role for this isoform in excitation-contraction coupling. In contrast, the role of RyR3 is unknown. We studied the participation of RyR3 in calcium release in wild type (containing both RyR1 and RyR3 isoforms) and RyR3−/− (containing only RyR1) myotubes in the presence or absence of imperatoxin A (IpTxa), a high-affinity agonist of ryanodine receptors. IpTxa significantly increased the amplitude and the rate of release only in wild-type myotubes. Calcium currents, recorded simultaneously with the transients, were not altered with IpTxa treatment. [^{3}H]ryanodine binding to RyR1 or RyR3 was significantly increased in the presence of IpTxa. Additionally, IpTxa modified the gating and conductance level of single RyR1 or RyR3 channels when studied in lipid bilayers. Our data show that IpTxa can interact with both RyRs and that RyR3 is functional in myotubes and it can amplify the calcium release signal initiated by RyR1, perhaps through a calcium-induced mechanism. In addition, our data indicate that when RyR3−/− myotubes are voltage-clamped, the effect of IpTxa is not detected because RyR1s are under the control of the dihydropyridine receptor.

INTRODUCTION

Ryanodine receptors (RyRs) are large tetrameric proteins involved in calcium release from intracellular stores. To date, three genes of RyRs have been identified (Sutko and Airey, 1996; Sorrentino et al., 2000). Expression of the three known RyRs varies in different tissues, suggesting unique functional attributes of each isoform essential for generating calcium signals (Giannini et al., 1992, 1995). Recent studies have shown that most skeletal muscles from adult mice contain only RyR1, with the exception of diaphragm, which expresses low levels of RyR3 (Conti et al., 1996). In contrast, all skeletal muscle from neonatal mice (Bertocchini et al., 1997) and myotubes in culture obtained from wild-type mice (Shirokova et al., 1999) contain both RyR1 and RyR3 isoforms.

In skeletal muscle, it is widely accepted that the RyR1 is directly activated by the dihydropyridine receptor (DHPR) during excitation-contraction (E-C) coupling. Previous studies have demonstrated that several portions of the cytoplasmic loop connecting repeats II and III of the DHPR α1 subunit bind to RyR1 (Leong and MacLennan, 1998), induce calcium release from the sarcoplasmic reticulum (El-Hayek et al., 1995; El-Hayek and Ikemoto, 1998), or are able to restore E-C coupling in dysgenic myotubes (Tanabe et al., 1990; Nakai et al., 1998). Moreover, a specific region of the II-III loop has been identified as the site for interaction between RyR1 and DHPR in situ (Proenza et al., 2000; Wilkens et al., 2001). The essential role of RyR1 in E-C coupling has been further supported by the finding that membrane depolarization fails to evoke calcium release in muscle cells lacking RyR1 (Takeshima et al., 1994). On the contrary, the role of RyR3 in calcium release during E-C coupling is still uncertain. In agreement with RyR3 expression in neonatal muscles, functional studies in wild-type and RyR3 knockout (RyR3−/−) mice demonstrated that contraction was significantly depressed in RyR3−/− muscle (Bertocchini et al., 1997). On the basis of these results, it has been suggested that RyR3 may contribute to amplification of calcium release generated by RyR1 (Bertocchini et al., 1997). Although initial studies have found no differences in calcium transients recorded in the presence or absence of RyR3 (Dietze et al., 1998), the interaction between RyR1 and RyR3 has been demonstrated by measuring calcium release in the form of sparks. The properties of sparks in RyR3−/− differ from those recorded from muscles containing both isoforms of RyRs (Conklin et al., 1999, 2000; Shirokova et al., 1999). In line with evidence of functional interactions between these channels, immunolocalization studies have revealed that RyR1 and RyR3 are co-localized in the triad junction (Flucher et al., 1999).

Imperatoxin A (IpTxa), a 33-amino acid peptide from the scorpion *Pandinus imperator*, has high affinity for RyR1 and RyR2 and has been reported to modify RyR-channel activity (Tripathy et al., 1998). At nanomolar concentrations, IpTxa induces the appearance of long-lived subconductance states (Tripathy et al., 1998). The molecular mechanism of IpTxa effect is unknown, but structural studies

Submitted June 12, 2001, and accepted for publication November 27, 2001.

Address reprint requests to Jesús García, MD, PhD, Department of Physiology and Biophysics, University of Illinois at Chicago College of Medicine, 900 South Ashland Avenue, Chicago, IL 60607. E-mail: garmar@uic.edu.

0006-3495/02/03/1319/10 $2.00

(Gurrola et al., 1999) suggest that IpTxa may mimic a portion of the II-III loop that activates RyRs. IpTxa decreases the amplitude and increases the duration of calcium sparks recorded from amphibian skeletal muscle (Shtifman et al., 2000; González et al., 2000), which contains both the α and β RyR isoforms. Because the amphibian α and β isoforms are homologous with the mammalian RyR1 and RyR3 types, respectively (Oyamada et al., 1994), that IpTxa may also interact with RyR3 is an attractive hypothesis.

We measured calcium transients and calcium currents in wild-type (containing both RyR1 and RyR3 isoforms) and RyR3−/− (containing only the RyR1 isoform) myotubes in the presence or absence of IpTxa. In wild-type myotubes, the amplitude of calcium transients and the rate of release were significantly increased in the presence of IpTxa, whereas the calcium current was unaffected. The changes in calcium transients were not observed in RyR3−/− myotubes. [^{3}H]ryanodine binding to sarcoplasmic reticulum vesicles prepared from wild-type or RyR3−/− microsomes was significantly increased in the presence of IpTxa. Additionally, the activity of single RyR channels was recorded in lipid bilayers. IpTxa modified the gating and conductance level of both RyR1 and RyR3 channels. Our data show that although IpTxa can interact with both RyR1 and RyR3 channels in single channel experiments and in [^{3}H]ryanodine binding, in intact myotubes the effects of IpTxa seem to be mainly mediated by RyR3 channels, as myotubes from RyR3−/− mice are poorly responsive to this toxin. In addition, the reported data are compatible with a model where RyR1s are controlled by DHPRs in voltage-clamped RyR3−/− myotubes and, because of this interaction, IpTxa does not modify the gating of RyR1s.

METHODS

Cell culture

Primary myoblasts were isolated from limb muscles of neonatal mice (postnatal day 0). Mice were obtained from a colony of homozygous RyR3-null (RyR3−/−; stock B6, 129P2-RyR3)(Bertocchini et al. 1997) and from a colony of mice containing both RyR1 and RyR3 (wild type; stock CACNA1SxNIHS-BCfBR). We have previously shown that myotubes derived from wild-type mice contain both RyR1 and RyR3 using immunofluorescence and confocal microscopy (Shirokova et al., 1999).

Muscles were finely minced and incubated for 30 min in rodent Ringer solution (in mM: 146 NaCl, 5 KCl, 2 $CaCl_2$, 1 $MgCl_2$, 11 glucose, 10 HEPES, pH 7.4) containing 0.3% trypsin and 0.01% DNase. The suspension was then centrifuged and filtered to remove large debris and then plated onto 35-mm Falcon Primaria dishes (Becton Dickinson Labware, Franklin Lakes, NJ) in plating media containing (v/v) 80% Dulbecco modified Eagle medium with 4.5 g/l glucose, 10% horse serum, and 10% calf serum. After 2 days, plating media was replaced with maintenance media: 90% Dulbecco modified Eagle medium, 10% horse serum. All cultures contained penicillin (100 U/ml) and streptomycin (100 mg/ml). Cultures were maintained at 37°C in a 95% air/5% CO_2, water-saturated atmosphere. Myotubes were studied 7–10 days after initial plating. At this time in culture, myotubes are multinucleated cells and contract vigorously, either spontaneously or after electrical stimulation (García and Beam, 1994). The size of the myotubes used in this study, as determined by cell capacitance, varied from 130 to 280 pF.

Electrophysiology and optical recording from myotubes

Measurements from myotubes were obtained using the patch-clamp or lipid bilayer techniques.

Patch clamp

Transmembrane currents were recorded using the whole-cell configuration of the patch-clamp method (Hamill et al. 1981). Patch pipettes were made from borosilicate glass and had resistances of 1.5 to 2.1 MΩ when filled with internal solution (mM: 145 Cs-aspartate, 10 HEPES, 5 $MgCl_2$, 10 Cs-EGTA, and 0.2 K_5Fluo-3, pH 7.4). IpTxa was added to the internal solution at a concentration of 10 μM. The external solution contained (mM): 145 tetraethylammonium chloride, 10 HEPES, 10 $CaCl_2$, and 0.003 tetrodotoxin. Analog compensation was used to reduce series resistance to charge the membrane with a time constant <1 ms. Cell capacitance, used to calculate the membrane current density (pA/pF), was measured by integrating the current evoked by a 10-mV hyperpolarization from a holding potential of −80 mV. Test currents were corrected for remaining components of linear capacitance and resistive current by digital scaling and subtraction of the average of eight control currents (García and Beam, 1994). L-type calcium currents were elicited with a prepulse protocol as described in Adams et al. (1990) to inactivate other voltage-dependent channels. In this protocol a 1-s prepulse to −30 mV is followed by a step to −50 mV for 25 ms, a 100-ms test step to potentials from −40 to 60 mV, back to −50 for 25 ms, and finally to a holding potential of −80 mV. To construct current-voltage relationships, the experimental data were fit to a Boltzmann equation: $I(V) = G_{maxL} \times (V - V_r)/(1 + \exp(V_L - V)/k_L)$ where $I(V)$ is the maximum calcium current at a given test potential; G_{maxL} is the maximum L-type channel conductance; V_r is the reversal potential for calcium; V is the test potential; V_L is the half-maximal activation potential for the L-type channel; and k_L is the slope factor.

Calcium transients were recorded simultaneously with the currents using Fluo-3 contained in the patch pipette. The filter combination consisted of a band-pass excitation filter centered at 470 nm (half bandwidth 20 nm), a dichroic long-pass mirror centered at 510 nm, and a long-pass emission filter centered at 520 nm. The background fluorescence for each myotube was measured and cancelled before entering whole cell mode. Fluorescence records are expressed as $\Delta F/F$, where $\Delta F = F_{transient} - F_{baseline}$ and F is $F_{baseline}$. Baseline fluorescence is the emissions recorded just before the start of a voltage step (García and Beam, 1994). The calcium transients were fit to the equation: $\Delta F/F = (\Delta F/F)_{max}/[1 + \exp\{(V_F - V)/k_F\}]$, where $(\Delta F/F)_{max}$ is the maximum fluorescence change; V_F is the potential that elicits half-maximal change in fluorescence; V is the test potential; and k_F is the slope factor for the fluorescence signal.

Lipid bilayer and analysis of single-channel data

Single-channel recordings of RyRs were performed by fusing microsomes of Chinese hamster ovary (CHO) cells expressing RyR3 or microsomes of rabbit skeletal muscle containing RyR1 into planar lipid bilayers. A mixture of phosphatidylserine: phosphatidylethanolamine (1:1 ratio), dissolved in *n*-decane at a concentration of 25 mg/ml, was used to form lipid bilayer membranes across a 250-μm aperture separating the *cis* side from the *trans* side. The *cis* chamber was the voltage control side whereas the *trans* side was held at virtual ground. The *cis* (600-μl) and *trans* (800-μl) chambers were initially filled with 50 mM Cs-methanesulfonate and 10 mM Tris/HEPES pH 7.2. After bilayer formation, a Cs-methanesulfonate gradient (300 mM *cis*/50 mM *trans*) was established. A Ca:EGTA mixture was then

added to the *cis* chamber from a 100-fold stock to reach a desired free [Ca^{2+}]. Free Ca^{2+} was calculated using the Ca:EGTA constants given in Fabiato and Fabiato (1979). Cellular microsomes were added to the *cis* chamber, which corresponded to the cytoplasmic side of the channel. After visualization of channel openings, Cs^{+} in the *trans* chamber was raised to 300 mM to collapse the chemical gradient and to prevent further vesicle insertion. Data were collected at steady voltages (+30 and −30 mV) for 2–5 min before and after IpTxa addition. Channel activity was recorded with a 16-bit videocassette recorder-based acquisition and storage system at a 10-kHz sampling rate. Signals were then analyzed after filtering with an 8-pole Bessel filter at a frequency of 1.5–2 kHz, as described (Tripathy et al., 1998).

[^{3}H]ryanodine binding assays

Measurements of [^{3}H]ryanodine binding were carried out as described earlier (Lokuta et al., 1997; Zhu et al., 1999). Briefly, microsomes of either wild-type or RyR3−/− myotubes were incubated for 90 min at 36°C with 7 nM [^{3}H]ryanodine in medium containing 0.2 M KCl, 10 mM Na-HEPES (pH 7.2), and 10 μM $CaCl_2$ in the absence and the presence of IpTxa. The microsomal protein concentration in the final reaction mixture was 30 to 50 μg. Nonspecific binding, amounting to 30–40% of the total binding, was determined in the presence of 20 μM unlabeled ryanodine and has been subtracted from the data presented. Samples (0.1 ml) were always run in duplicate or triplicate, filtered onto glass fiber filters (Whatman GF/B or GF/C) and washed twice with 5 ml of cold water using a Brandel M-24R cell harvester (Gaithersburg, MD). The filters were placed in scintillation vials and the retained radioactivity measured in a Beckman LS-5000 TD β-counter (Beckman Instruments, Fullerton, CA).

Statistics

Calcium transient and calcium current data were analyzed for statistical significance with Statistica 5 (StatSoft, Tulsa, OK) using analysis of variance with repeated measurements. Comparisons between binding data groups were assessed with Origin 6.0 (Microcal Software, Northampton, MA) using an unpaired Student's *t* test. A P value < 0.05 was considered to be statistically significant.

RESULTS

Effect of IpTxa on calcium transients in skeletal myotubes

A prepulse protocol was used to measure calcium transients elicited by activation of DHPRs. With this protocol calcium transients are not contaminated with calcium entry through the T-type calcium channel (García and Beam, 1994). Calcium transients were recorded from wild-type and RyR3−/− myotubes in the absence and the presence of 10 μM IpTxa. Transients from wild-type myotubes had characteristics similar to those recorded from RyR3−/− myotubes in the absence of IpTxa, in agreement with a previous study by Dietze et al. (1998). A representative trace of each group of myotubes is shown in Fig. 1 *A* for a pulse to +20 mV. The similarity of the calcium transients between the two groups persisted for a period of 40 min, which was the maximum time we were able to record reliable calcium transients from these cells. After this time, the levels of calcium between command pulses increase substantially and the decay of the transients becomes slower.

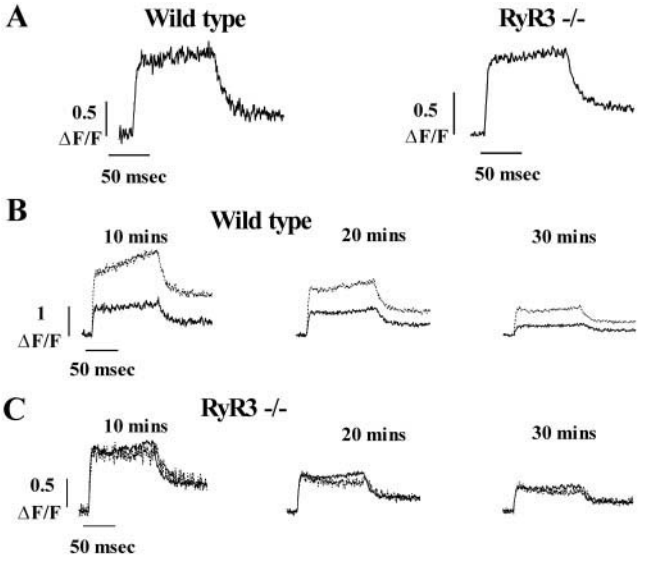

FIGURE 1 IpTxa enhances peak calcium transient amplitude in wild-type but not RyR3−/− myotubes. (*A*) Typical calcium transient waveforms elicited by a pulse to +20 mV from wild type (*left*) and RyR3 −/− (*right*). (*B*) Calcium transients recorded from wild-type myotubes 10, 20, and 30 min after entering whole-cell recording mode. Note the difference in amplitude when comparing cells treated with IpTxa (*dotted line*) and without IpTxa (*continuous line*). (*C*) Transients recorded from RyR3−/− myotubes 10, 20, and 30 min after entering whole-cell recording mode. Unlike the transients recorded from wild type, there is no difference between cells treated with IpTxa (*dotted line*) and control cells (*continuous line*). For both, wild-type and RyR3−/− myotubes, the records in the presence or absence of the toxin were obtained from different cells. Calcium transients were recorded using the prepulse protocol described in the Methods section.

The amplitude of the transients increased significantly in wild-type myotubes when the cells were perfused internally with IpTxa. The difference in amplitude between IpTxa-treated and -untreated wild-type myotubes was apparent as early as 10 min after attaining whole-cell mode, suggesting a gradual penetration of the peptide toxin into the cell. We did not attempt to record transients before 10 min because the calcium-sensitive dye Fluo-3 was included in the patch pipette and it also has to diffuse into the cell. The change in amplitude of the transient suggests that IpTxa reached, and interacted with, RyRs by this time. In fact, the relative increase in calcium transient amplitude became even larger as myotubes were exposed to the toxin for longer times. Records in Fig. 1 *B* show the increase in amplitude as a function of time for a control and an IpTxa-treated wild-type myotube. It can be seen that IpTxa increased the calcium transient in the wild-type treated myotube despite the rundown of the transients commonly observed in untreated myotubes. Thus, the increase of the calcium transient in the presence of IpTxa represents a lower limit of this effect. The increase in calcium transient in the presence of

TABLE 1 Properties of calcium transients in wild type and RyR3−/− myotubes

Time	Group	$\Delta F/F_{max}$	k_F (mV)	V_F (mV)	$d[\Delta F/F]/dt_{max}$	n
10 min	Wild type	1.19 ± 0.21	4.77 ± 0.18	−0.51 ± 0.74	0.17 ± 0.03	15
	Wild type + IpTxa	1.94 ± 0.34*	3.54 ± 0.38	−3.40 ± 1.74*	0.27 ± 0.04*	13
	RyR3−/−	0.99 ± 0.16	6.31 ± 1.32	−0.10 ± 1.22	0.14 ± 0.02	17
	RyR3−/− + IpTxa	1.34 ± 0.23	3.57 ± 0.35	−1.48 ± 0.54	0.17 ± 0.04	13
20 min	Wild type	0.68 ± 0.12	4.60 ± 0.26	−1.06 ± 0.79	0.10 ± 0.02	13
	Wild type + IpTxa	1.71 ± 0.29*	3.74 ± 0.54	−4.94 ± 2.19*	0.22 ± 0.04*	8
	RyR3−/−	0.71 ± 0.13	4.40 ± 0.18	−1.40 ± 1.16	0.09 ± 0.01	13
	RyR3−/− + IpTxa	0.68 ± 0.09	3.85 ± 0.23	−2.25 ± 0.58	0.12 ± 0.02	10
30 min	Wild type	0.40 ± 0.18	4.58 ± 0.23	−1.93 ± 1.76	0.06 ± 0.03	4
	Wild type + IpTxa	1.16 ± 0.20*	3.49 ± 0.26	−5.64 ± 2.07*	0.16 ± 0.03*	6
	RyR3−/−	0.54	4.44	2.06	0.07	2
	RyR3−/− + IpTxa	0.40 ± 0.09	3.82 ± 0.20	−3.51 ± 2.56	0.05 ± 0.01	6

Control and IpTxa-treated wild-type cells are shown at the top half of each time point; RyR3−/− myotubes under control and toxin-treated conditions are shown at the bottom half. Values in each column are averages ± SE. *n* represents the number of cells examined in each group. Note that for the control group of RyR3−/− we examined only two cells and no SE is given and no comparisons were made with treated cells. The asterisk indicates that the toxin-treated group had a statistically significant difference with the corresponding control group (*P* value <0.05). No statistically significant differences were found between controls of wild-type and RyR3−/− myotubes, or between control and toxin-treated RyR3−/− myotubes.

IpTxa was not present in RyR3−/− myotubes. Fig. 1 *C* compares calcium release in a typical control and toxin-treated cells. It shows clearly that IpTxa does not enhance calcium release in RyR3−/− myotubes. Thus, these data indicate that only myotubes containing the type 3 RyR respond to internal application of IpTxa with an increase in calcium release. The third column in Table 1 corresponds to the maximum amplitude of the transients at 10, 20, and 30 min for the different groups of cells.

In addition to increasing the amplitude of the calcium transient, IpTxa also caused a small but statistically significant shift of the voltage dependence of activation of the calcium transient to more negative potentials in wild-type myotubes but not in RyR3−/−. The graphs in Fig. 2 show the voltage dependence of the calcium transient amplitude recorded from wild-type myotubes or RyR3−/− myotubes at 10 (*A*), 20 (*B*), and 30 (*C*) min after entering the whole-cell mode. Transients recorded from untreated myotubes are represented by triangles and those recorded in the presence of IpTxa are represented by squares. The difference in the curves is evident for wild-type myotubes, whereas the curves corresponding to RyR3−/− myotubes overlap almost entirely. The average values of V_F and k_F for wild-type and RyR3−/− myotubes are shown in columns 4 and 5 of Table 1. The changes observed in wild-type myotubes may be explained by an amplification of calcium release mediated by RyR3, as previously suggested by Bertocchini et al. (1997).

IpTxa increases the rate of calcium release

We next determined the rate of calcium release by calculating the derivative of the transient with respect to time. The derivative represents an accurate approximation of the rate of release in myotubes because these cells have a negligible calcium removal flux (García and Beam, 1994), and furthermore, as shown by Ríos and Pizarro (1991), the removal flux can be neglected if a large concentration of calcium buffers is present in the sarcoplasm. In our experiments, the intracellular solution contained 1 mM EGTA and 0.2 mM Fluo-3, which represent a high concentration of calcium buffers in these cells. In addition, Schuhmeier and Melzer (2001) have recently validated this method for cultured myotubes. Typical traces of the calcium transient derivative for each group of myotubes are shown in Fig. 3 *A*. IpTxa significantly increased the value of the derivative in wild-type myotubes, indicating a larger rate of release. In contrast, the rate of release was not modified in RyR3−/− in the presence of IpTxa. The average of the maximum values of the derivatives is shown in column 6 of Table 1.

The graphs in Fig. 3, *B–D* show the voltage dependence of the derivative at 10, 20, and 30 min of recording, respectively. The voltage dependence of the derivative was similar in all groups and at all times, except for the increase in amplitude of the wild-type group treated with IpTxa. The amplitude of the derivative in wild-type myotubes was similar to the amplitude of untreated and IpTxa-treated RyR3−/− myotubes. Thus, these data strongly suggest that RyR3 mediates the increase in the rate of calcium release. The lack of effect of IpTxa on RyR1 was surprising, considering the marked effect of the toxin on isolated RyR1 channels (Tripathy et al., 1998; Gurrola et al., 1999). However, in current models of E-C coupling, RyR1 is in direct contact with the voltage sensors of T-tubules. Therefore, it is conceivable that the physical connection of RyR1 to the voltage sensors prevents the effect of IpTxa by hindering access to its binding site.

IpTxa does not modify L-type calcium currents

The II-III loop of α1S interacts with RyR1 (Tanabe et al., 1990; El-Hayek et al., 1995; Nakai et al., 1996). Apart from its well known function in triggering the release of calcium

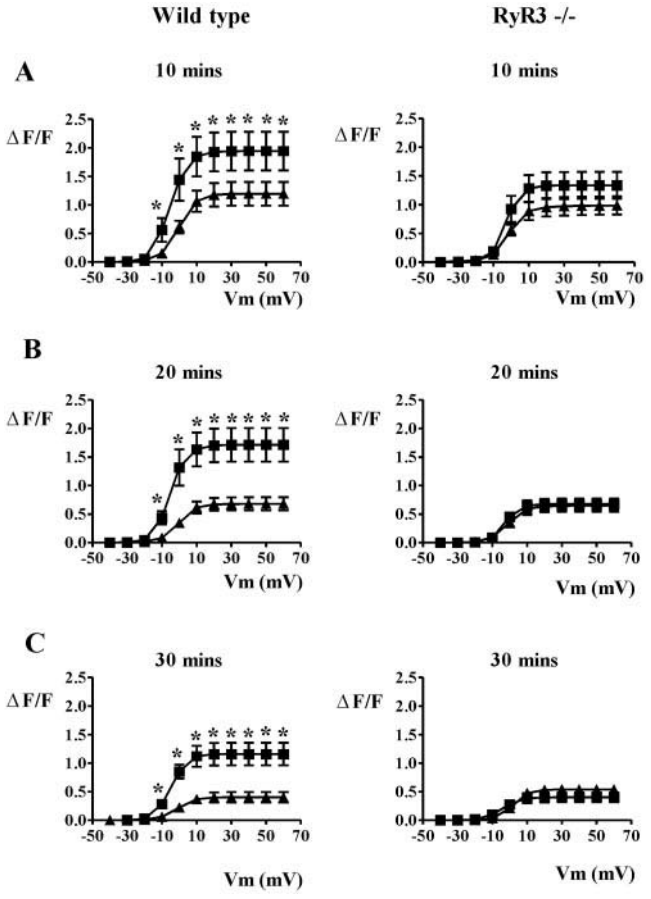

FIGURE 2 IpTxa increases calcium transient amplitude in wild-type but not RyR3−/− skeletal myotubes. *A–C* show the voltage dependence of the peak calcium transient amplitude for wild type (*left*) and RyR3−/− (*right*). Transients were recorded 10 (*A*), 20 (*B*), and 30 (*C*) min after entering the whole-cell configuration. The curves through the experimental data correspond to the fitting of the equation described in Methods and used to obtain the voltage dependence parameters of the transients, shown in Table 1. Statistically significant differences ($P < 0.05$) are denoted by an asterisk for comparisons between treated (■) and untreated (▲) myotubes.

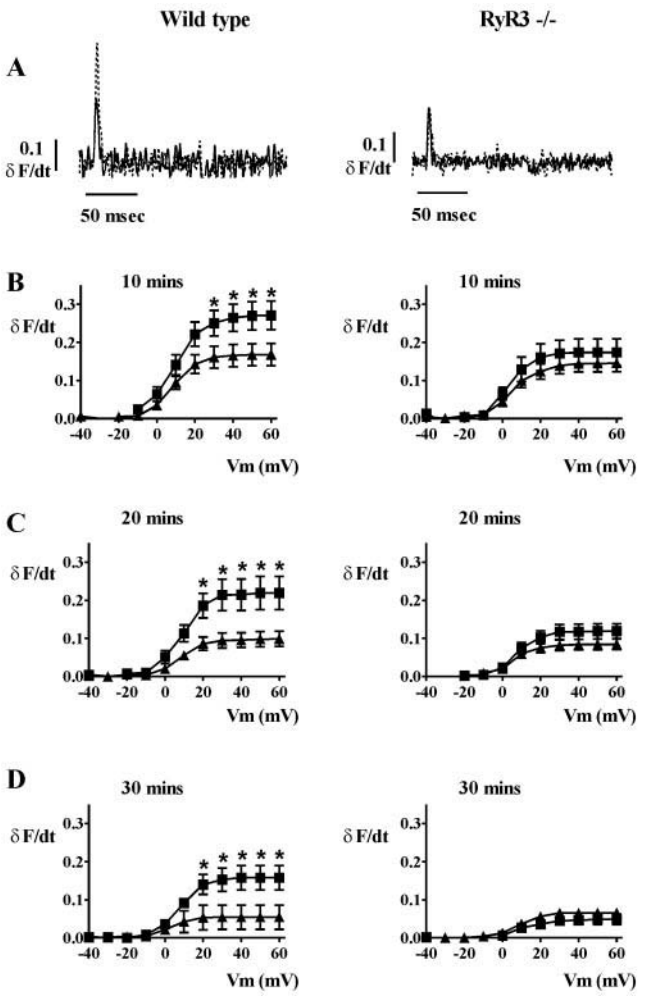

FIGURE 3 IpTxa increases the amplitude of the first derivative of the calcium transient in wild type but not in RyR3−/− skeletal myotubes. *A* shows the derivative of a typical calcium transient elicited by a test pulse to +20 mV recorded from a wild-type (*left*) and an RyR3−/− (*right*) myotube. The continuous line corresponds to untreated myotubes and the dashed line corresponds to treated cells. *B–D* show the voltage dependence of the calcium transient derivative for wild type (*left*) and RyR3−/− (*right*) at different times after attaining whole-cell mode. Statistically significant differences ($P < 0.05$) are denoted by an asterisk. Data from control myotubes are represented by triangles, whereas the squares represent data from toxin-treated myotubes in each group.

from intracellular stores, the interaction between the II-III loop and RyR1 enhances currents through the L-type calcium channel (Nakai et al., 1996). Because IpTxa may be structurally related to an active segment of the II-III loop, we measured L-type calcium currents in cells perfused with the toxin and compared them with those recorded from unperfused cells to find out whether IpTxa affects the cross-talk between RyR1 and the L-type calcium channel.

Representative traces of calcium currents obtained at +20 mV are shown in Fig. 4 *A*. Calcium currents had similar kinetics and amplitude in wild-type and RyR3−/− myotubes in control conditions or in the presence of IpTxa. Comparison of the current-voltage relationships (Fig. 4, *B–D*) shows that IpTxa did not modify the voltage dependence of the calcium current at any time point. The experimental data were fitted as explained in the Methods section to obtain the different parameters in columns 3–6 of Table 2. None of those parameters were different between treated and untreated groups. Thus, our results indicate that IpTxa alters calcium release but does not affect the RyR1-mediated L-type current enhancement.

Increase of ryanodine binding by IpTxa

To determine whether the difference in calcium release between wild type and RyR3−/− in the presence of IpTxa was attributable to a lack of interaction of the toxin in RyR3−/− myotubes, (1) microsomal preparations were

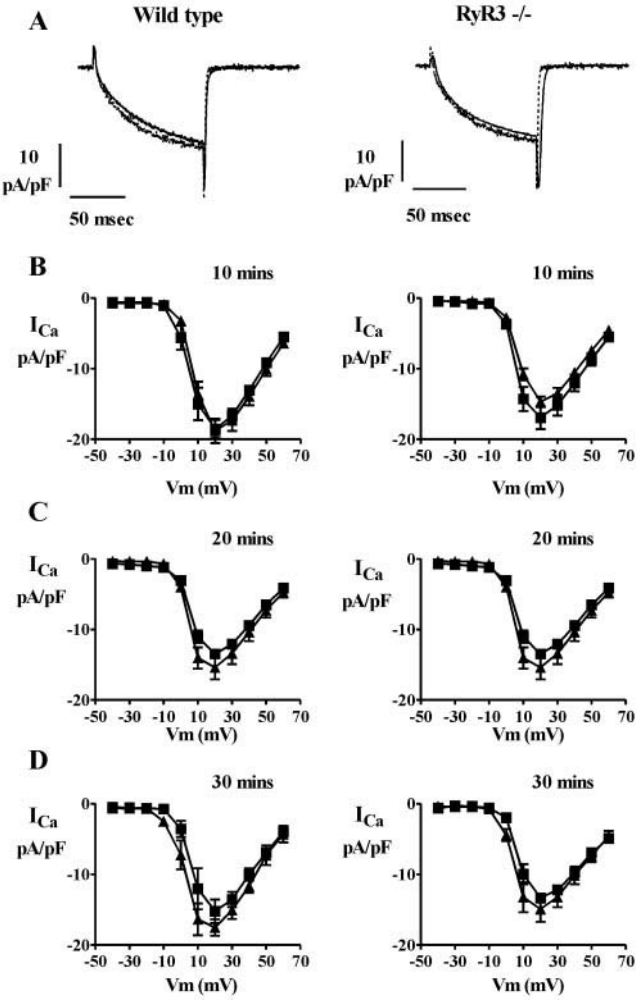

FIGURE 4 IpTxa does not affect L-type calcium currents in skeletal myotubes. *A* shows representative traces of calcium currents recorded from wild-type (*left*) or RyR3−/− (*right*) myotubes in the absence (*continuous line*) or the presence (*dashed line*) of IpTxa. (*B—D*) Comparison of voltage dependence and amplitude of calcium currents recorded from wild-type and RyR3−/− myotubes with and without IpTxa. The peak amplitude of the calcium current is plotted as a function of voltage. Currents were recorded 10 (*B*), 20 (*C*), and 30 (*D*) min after entering the whole-cell recording mode. No statistically significant difference was found between any group at any time. The values of maximum conductance and voltage dependence of calcium currents are shown in Table 2. Calcium currents were recorded simultaneously with calcium transients using a prepulse protocol. Control values are represented by triangles and values from toxin-treated cells are represented by squares.

obtained from both types of myotubes and (2) [^{3}H]ryanodine binding was measured in the presence of IpTxa.

Microsomes were incubated for 90 min at 36°C with 7 nM [^{3}H]ryanodine in medium containing 0.2 M KCl, 10 mM Na-HEPES (pH 7.2). At a free [Ca^{2+}] ≤10 nM (1 mM EGTA and no $CaCl_2$ added), no specific binding was detected. In the presence of 10 μM free [Ca^{2+}], specific binding increased to 90–290 fmoles/mg protein. This value represents the control [^{3}H]ryanodine binding and was used to normalize the binding in the presence of IpTxa for each microsomal preparation. Normalization of [^{3}H]ryanodine was necessary to account for the differences in the number of cells of each culture and thus the amount of total protein and RyRs. Fig. 5 shows that, in the presence of IpTxa, binding increased significantly ($P < 0.05$) to 245 ± 8.1% ($n = 6$) in wild-type myotubes and 238 ± 8.9% ($n = 5$) in RyR3−/− myotubes compared with control. These results indicate that the binding properties of RyRs in wild-type and RyR3−/− myotubes are similar.

Single RyR activity recorded in lipid bilayers

Because [^{3}H]ryanodine binding using microsomal preparations does not indicate whether IpTxa modulates RyR3 specifically, we studied the effect of IpTxa on RyR3s, separately from RyR1s. To obtain a pure population of RyR3s, channels were expressed in CHO cells and subsequently isolated in microsomal vesicles. We and others have previously shown that CHO cells do not express detectable amounts of endogenous RyRs when assayed by Western blots, Northern blots, or ryanodine binding (Pan et al., 2000; Xu et al., 2000; Gurrola et al., 1999). RyR1 channels were obtained from rabbit skeletal muscle vesicles. The activity of the channels was recorded after reconstitution of the vesicles in lipid bilayers. Channels were activated with 10 μM free [Ca^{2+}] added to the *cis* chamber (cytosolic side of the channels). Single channel recordings are shown in Fig. 6 *A*. The upper traces show the steady-state channel activity elicited by Ca^{2+}. Approximately 1 min after the addition of 100 nM IpTxa to the *cis* chamber, a long-lived subconductance state appeared in both RyR1 and RyR3 channels. The subconductance level was 30% of the full amplitude and is very similar to the behavior reported for adult skeletal and cardiac RyRs (Tripathy et al., 1998) and for frog RyRs (Shtifman et al., 2000). Bursts of full-conductance openings, corresponding to IpTxa dissociation from the channel, were regularly observed in both channels (Fig. 6 *A*, lower panels). These effects of IpTxa have been postulated to occur as a result of the reversible binding of the toxin to a single site in the cytoplasmic side of the channel that is different from the ryanodine binding site (Tripathy et al., 1998). The graphs in Fig. 6 *B* show the single channel amplitude as a function of voltage. The slope of the curves, which represents channel conductance, was less steep in the presence of the toxin (●) compared with control (○). This result demonstrates that IpTxa interacts with RyR3 and supports the idea that IpTxa induces a functional modification of RyR3, which may explain the increase in calcium release observed in wild-type myotubes.

TABLE 2 Properties of calcium currents in wild type and RyR3-/- myotubes

Time	Group	$Gmax_L$ (nS/nF)	k_L (mV)	V_L (mV)	Vr (mV)	n
10 mins	Wild type	339 ± 22.6	4.7 ± 0.4	9.8 ± 0.8	77.1 ± 1.0	15
	Wild type + IpTxa	323 ± 27.7	4.3 ± 0.6	8.2 ± 1.9	76.0 ± 1.7	13
	RyR3−/−	314 ± 15.5	4.4 ± 0.3	8.8 ± 0.9	74.5 ± 0.8	17
	RyR3−/− + IpTxa	258 ± 35.8	4.2 ± 0.7	7.7 ± 1.4	78.0 ± 1.7	13
20 mins	Wild type	344 ± 34.9	4.8 ± 0.3	9.4 ± 1.1	72.0 ± 1.1	13
	Wild type + IpTxa	319 ± 30.0	4.5 ± 0.3	7.0 ± 2.5	74.4 ± 2.2	
	RyR3−/−	288 ± 19.6	4.8 ± 0.3	8.1 ± 1.0	74.7 ± 1.3	13
	RyR3−/− + IpTxa	260 ± 23.0	4.3 ± 0.2	7.3 ± 0.9	75.1 ± 1.6	10
30 mins	Wild type	353 ± 6.1	4.1 ± 0.4	5.9 ± 0.8	70.2 ± 1.6	4
	Wild type +IpTxa	345 ± 59.7	4.4 ± 0.5	7.6 ± 2.4	75.9 ± 1.5	6
	RyR3−/−	262	4.3	9.1	76.7	2
	RyR3−/− + IpTxa	324 ± 38.1	4.0 ± 0.5	6.24 ± 1.2	77.1 ± 2.9	6

Calcium currents were recorded simultaneously with calcium transients using the prepulse protocol described in the Methods section. Values under each column represent averages ± SEM of the number of cells indicated in the last column.

DISCUSSION

Previous studies have determined the presence of RyR1 and RyR3 in embryonic and young animal skeletal muscles (Bertocchini et al., 1997), where these channels are co-localized at the junctional triad (Flucher et al., 1999). In addition, we have previously shown that RyR1 and RyR3 are expressed in cultured myotubes obtained from wild-type mice (Shirokova et al., 1999). Further evidence has revealed that expression of RyR3 is necessary for optimal muscle contraction in neonatal skeletal muscle (Bertocchini et al., 1997) and that co-expression of RyR1 and RyR3 isoforms is necessary to generate localized Ca^{2+} release events in myotubes (Conklin et al., 1999, 2000; Shirokova et al., 1999). Analysis of muscle preparations from RyR3−/− mice has revealed that caffeine sensitivity is strongly decreased compared with wild-type mice (Bertocchini et al., 1997; Rossi et al., 2001). Because RyR3 channels are apparently less abundant than RyR1 channels in neonatal muscles, it has been suggested that RyR3 channels contribute to E-C coupling through a calcium-induced calcium release mechanism,

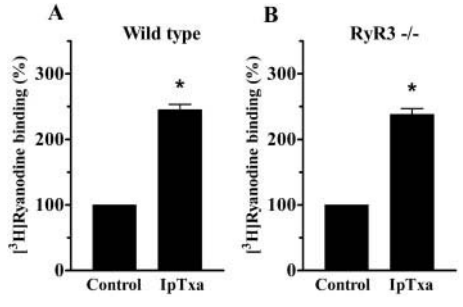

FIGURE 5 Effect of IpTxa on the binding of [^{3}H]ryanodine to wild-type and RyR3 knockout microsomes. The specific binding value in the presence of 10 μM free [Ca^{2+}] was 90–290 fmoles/mg protein. The specific value represents 100% binding for each microsomal preparation and was used to normalize the binding in the presence of 1 μM IpTxa. IpTxa increased [^{3}H]ryanodine binding in both preparations to the same extent. Binding was measured in the same preparation before and after the addition of IpTxa in six cases of microsomes from wild-type myotubes and five cases of RyR3−/− microsomes.

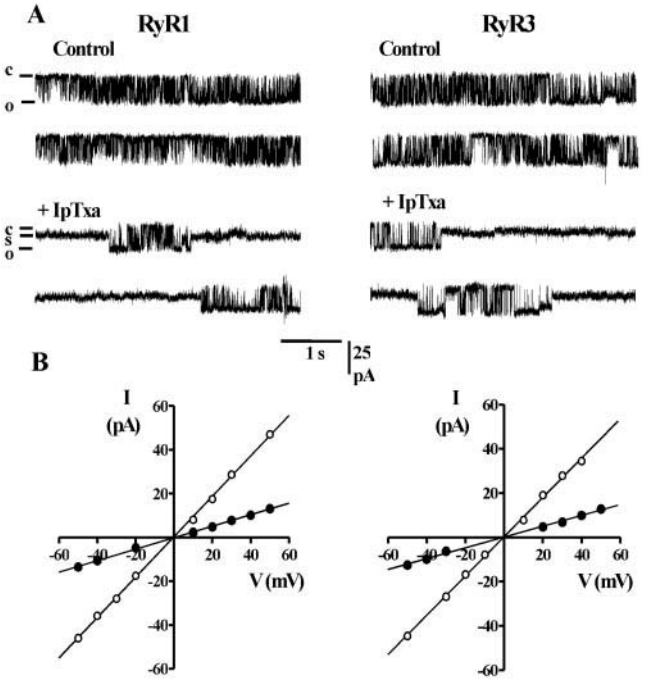

FIGURE 6 IpTxa induces the appearance of subconductance states in RyR1 and RyR3 channels. (*A*) Microsomal vesicles from rabbit skeletal muscle (labeled RyR1) and from CHO cells expressing RyR3 (labeled RyR3) were fused to lipid bilayers in the presence of 10 μM free [Ca^{2+}] in the *cis* chamber (cytosolic side of the channel) to activate RyR channels. The upper traces in each set represent the steady-state channel activity elicited by Ca^{2+}. The bottom traces show the same channels ~1 min after the addition of 100 nM IpTxa to the *cis* (cytosolic side) chamber. Records are representative of 15 preparations for RyR1 and 3 preparations for RyR3. (*B*) Current-voltage relationships for RyR1 (*left*) and RyR3 (*right*) in the absence of IpTxa (full conductance state; labeled control; ○) and for the IpTxa-induced subconductance state (+ IpTxa; ●). Slope conductance was 0.918 and 0.244 nS for RyR1 control and +IpTxa, respectively, and 0.898 and 0.239 nS for RyR3 control and +IpTxa, respectively.

whereas RyR1 channels are mainly controlled by voltage (Sorrentino and Reggiani, 1999). Yet, how RyR3 channels contribute to calcium signaling in neonatal skeletal muscle cells remains unclear.

In this paper we report that IpTxa, a high-affinity modulator of RyRs, increases the amplitude of the calcium transient and the rate of release in myotubes containing both RyR1 and RyR3, but not in myotubes from RyR3−/− mice which contain RyR1 only. However, IpTxa induces similar gating changes of RyR1 and RyR3 when examined in artificial lipid bilayers. Furthermore, IpTxa does not modify the L-type calcium currents in either kind of myotubes. Taken together, these results suggest that RyR1 channels in intact myotubes are not susceptible to the stimulatory effects of IpTxa.

Because the myotubes were obtained from mice with dissimilar genetic background, the possibility exists that the observed differences between wild-type and RyR3−/− cells was attributable to the genetic variation and not to the presence or absence of RyR3. However, this is a remote possibility as the proteins involved in E-C coupling are highly conserved. Perturbations in highly conserved sequences would have a greater impact on cellular function than genetic drift commonly seen in unconserved sequences such as introns.

Although IpTxa failed to modify all the measured parameters of calcium release in RyR3−/− myotubes (Figs. 1–3), data from [^{3}H]ryanodine binding experiments using microsomes (Fig. 5) or from analysis of single channels reconstituted in lipid bilayers (Fig. 6) show that IpTxa can markedly affect both RyR1 and RyR3 channels. The lack of effect of IpTxa on RyR3−/− myotubes could be explained by the tight control of RyR1 exerted by the DHPRs. In this case, the DHPR would command the RyR1 to open in a voltage-dependent manner and independent of IpTxa binding. This idea agrees with the fact that sparks are readily detected in skinned mammalian muscle cells (Kirsch et al., 2001) but not in intact, voltage-clamped adult cells or intact myotubes (Shirokova et al., 1998, 1999), which suggests RyR1 gating is under strict control of the DHPR. With this model of control of calcium release, sparks observed both in permeabilized (Shtifman et al., 2000; González et al., 2000) or intact, voltage-clamped frog muscle cells (Shirokova et al., 1998) could be explained by the presence of the β-RyR isoform, which, as we observed in mammalian myotubes, remains available to IpTxa effects, regardless of DHPRs. Based on the idea that RyR1 are under the control of DHPRs, our results also predict that IpTxa would not alter calcium release in adult mammalian skeletal muscle cells containing RyR1 only.

When RyR1 and RyR3 were studied separately in lipid bilayers, we found that IpTxa modified the conductance of both channels in a strikingly similar manner (Fig. 6). Furthermore, this effect was also similar to changes in gating previously observed in RyR2 in the presence of IpTxa (Tripathy et al., 1998), indicating a common functional response of all known mammalian RyRs. Interestingly, the response to IpTxa seems to be conserved between mammalian and frog RyRs, because frog RyRs show similar changes in gating (Shtifman et al., 2000). Thus, these data support a close correspondence between mammalian and frog RyR isoforms. These data, together with the changes observed on calcium sparks promoted by IpTxa (increased duration with lower amplitude), suggest that the underlying cause for the increase in calcium transients seen in wild-type myotubes is the longer opening of RyR3s. As all our experiments were conducted in voltage-clamped myotubes, it would be interesting to study the effect of IpTxa in permeabilized RyR3−/− myotubes. A hypothesis suggested by our study is that in permeabilized RyR3−/− myotubes, IpTxa may induce an increase of calcium sparks frequency because RyRs are not tightly controlled by DHPRs.

Because IpTxa increased the amplitude of the calcium transient and the rate of release in myotubes containing both RyR1 and RyR3, our results are compatible with an E-C coupling model where RyR3 amplifies the calcium signal initiated by RyR1s coupled to DHPRs. This amplification mechanism of calcium release is more prominent during the early upstroke of the calcium transient and decreases or inactivates with time during the course of a voltage step. In our scheme, the contribution of this mechanism would be absent during repolarization, thus explaining the fact that the decay of the transients was not modified in wild-type myotubes in the presence of IpTxa.

Another interesting finding coming from our experiments was that IpTxa did not modify the L-type calcium currents. It has been previously shown that the coupling between DHPRs and RyR1s enhances L-type calcium currents (Nakai et al., 1996). In dyspedic myotubes, which lack RyR1s, calcium currents are very small. Expression of RyR1s in dyspedic cells restores L-type current amplitude to levels found in normal myotubes. In our experiments, the properties of the recorded calcium currents from control or toxin-treated myotubes were similar. This suggests that IpTxa binding does not modify the DHPR-RyR1 interaction.

Our results support the idea that muscle cells can regulate E-C coupling through expression and assembly of different RyRs. This effect may be mediated through sideways interactions between calcium release channels (Marx et al., 1998) or through forward interactions between DHPRs and RyRs (Shirokova et al., 1999). Control of calcium release in mammalian skeletal muscle is thought to be compartmentalized into voltage-sensitive and -insensitive sites (Shirokova et al., 1998). Furthermore, it has been shown that extrajunctional rows of RyRs form only in skeletal muscle that expresses both RyR1 and RyR3. (Felder and Franzini-

Armstrong, 2001). Thus, the arrangement of RyRs is affected by expression of different RyR gene products. Interestingly, RyR3 and RyR1/2 also have different localization patterns in smooth muscle and distinct functions in E-C coupling (Mironneau et al., 2001). Therefore, differential expression and assembly of calcium release channels may be an important mechanism regulating E-C coupling in muscle cells.

This work was supported by grants from the National Science Foundation (J.G.), the National Institutes of Health (HL47053 and HL55438 to H.V.), and Telethon (1151), MURST, and AIRC (V.S.). H.H.V. is an Established Investigator of the American Heart Association.

REFERENCES

Adams, B. A., T. Tanabe, A. Mikami, S. Numa, and K. G. Beam. 1990. Intramembrane charge movement restored in dysgenic skeletal muscle by injection of dihydropyridine receptor cDNAs. *Nature.* 346:569–572.

Bertocchini, F., C. E. Ovitt, A. Conti, V. Barone, H. R. Scholer, R. Bottinelli, C. Reggiani, and V. Sorrentino. 1997. Requirement for the ryanodine receptor type 3 for efficient contraction in neonatal skeletal muscles. *EMBO J.* 16:6956–6963.

Conklin, M. W., P. Powers, R. Gregg, and R. Coronado. 1999. Contribution of ryanodine receptor type 3 to Ca^{2+} sparks in embryonic mouse skeletal muscle. *Biophys. J.* 77:1394–1403.

Conklin, M. W., C. A. Ahern, P. Vallejo, V. Sorrentino, H. Takeshima, and R. Coronado. 2000. Comparison of Ca^{2+} sparks produced independently by two ryanodine receptor isoforms (type 1 or type 3). *Biophys. J.* 78:1777–1785.

Conti, A., L. Gorza, and V. Sorrentino. 1996. Differential distribution of ryanodine receptor type 3 (RyR3) gene product in mammalian skeletal muscles. *Biochem. J.* 316:19–23.

Dietze, B., F. Bertocchini, V. Barone, A. Struk, V. Sorrentino, and W. Melzer. 1998. Voltage-controlled Ca^{2+} release in normal and ryanodine receptor type 3 (RyR3)-deficient mouse myotubes. *J. Physiol.* 513:3–9.

El-Hayek, R., B. Antoniu, J. Wang, S. L. Hamilton, and N. Ikemoto. 1995. Identification of calcium release triggering and blocking regions of the II-III loop of the skeletal muscle dihydropyridine receptor. *J. Biol. Chem.* 270:22116–22118.

El-Hayek, R., and N. Ikemoto. 1998. Identification of the minimum essential region in the II-III loop of the dihydropyridine receptor α 1 subunit required for activation of skeletal muscle-type excitation-contraction coupling. *Biochemistry.* 37:7015–7020.

Fabiato, A., and F. Fabiato. 1979. Calculator programs for computing the composition of the solutions containing multiple metals and ligands used for experiments in skinned muscle cells. *J. Physiol.* 75:463–505.

Felder, E., and C. Franzini-Armstrong. 2001. Possible parajunctional location of RyR3 in skeletal muscle. *Biophys. J.* 80:382A.

Flucher, B. E., A. Conti, H. Takeshima, and V. Sorrentino. 1999. Type 3 and type 1 ryanodine receptors are localized in triads of the same mammalian skeletal muscle fibers. *J. Cell Biol.* 146:621–629.

García, J., and K. G. Beam. 1994. Measurement of calcium transients and slow calcium currents in myotubes. *J. Gen. Physiol.* 103:107–123.

Giannini, G., E. Clementi, R. Ceci, G. Marziali, and V. Sorrentino. 1992. Expression of a ryanodine receptor-Ca^{2+} channel that is regulated by TGF-β. *Science.* 257:91–94.

Giannini, G., A. Conti, S. Mammarella, M. Scrobogna, and V. Sorrentino. 1995. The ryanodine receptor/calcium release channel genes are widely and differentially expressed in murine brain and peripheral tissues. *J. Cell Biol.* 128:893–904.

González, A., W. G. Kirsch, N. Shirokova, G. Pizarro, G. Brum, I. N. Pessah, M. D. Stern, H. Cheng, and E. Rios. 2000. Involvement of multiple intracellular release channels in calcium sparks of skeletal muscle. *Proc. Natl. Acad. Sci. U.S.A.* 97:4380–4385.

Gurrola, G. B., C. Arevalo, R. Sreekumar, A. J. Lokuta, J. W. Walker, and H. H. Valdivia. 1999. Activation of ryanodine receptors by imperatoxin A and a peptide segment of the II-III loop of the dihydropyridine receptor. *J. Biol. Chem.* 274:7879–7886.

Hamill, O. P., A. Marty, E. Neher, B. Sakman, and F. J. Sigworth. 1981. Improved patch-clamp techniques for high resolution recording from cells and cell-free membrane patches. *Pflugers Arch.* 391:85–100.

Kirsch, W. D., D. Uttenweiler, A. Both, A. González, E. Ríos, and R. H. Fink. 2001. Elementary Ca^{2+} release events in skinned fibers of adult mammalian skeletal muscle. *Biophys. J.* 80:65A.

Leong, P., and D. H. MacLennan. 1998. A 37-amino acid sequence in the skeletal muscle ryanodine receptor interacts with the cytoplasmic loop between domains II and III in the skeletal muscle dihydropyridine receptor. *J. Biol. Chem.* 273:7791–7794.

Lokuta, A. J., M. B. Meyers, P. R. Sander, G. Fishman, and H. H. Valdivia. 1997. Modulation of cardiac ryanodine receptors by sorcin. *J. Biol. Chem.* 272:25333–25338.

Marx, S. O., K. Ondrias, and A. R. Marks. 1998. Coupled gating between individual skeletal muscle Ca^{2+} release channels (ryanodine receptors). *Science.* 281:818–821.

Mironneau, J., F. Coussin, L. H. Jeyakumar, S. Fleischer, C. Mironneau, and N. Macrez. 2001. Contribution of ryanodine receptor subtype 3 to Ca^{2+} responses in Ca^{2+}-overloaded cultured rat portal vein myocytes. *J. Biol. Chem.* 276:11257–11264.

Nakai, J., R. T. Dirksen, H. T. Nguyen, I. N. Pessah, K. G. Beam, and P. D. Allen. 1996. Enhanced dihydropyridine receptor channel activity in the presence of ryanodine receptor. *Nature.* 380:72–75.

Nakai, J., T. Tanabe, T. Konno, B. Adams, and K. G. Beam. 1998. Localization in the II-III loop of the dihydropyridine receptor of a sequence critical for excitation-contraction coupling. *J. Biol. Chem.* 273:24983–24986.

Oyamada, H., T. Murayama, T. Takagi, M. Iino, N. Iwabe, T. Miyata, Y. Ogawa, and M. Endo. 1994. Primary structure and distribution of ryanodine-binding protein isoforms of the bullfrog skeletal muscle. *J. Biol. Chem.* 269:17206–17214.

Pan, Z., D. Damron, A. L. Nieminen, M. B. Bhat, and J. Ma. 2000. Depletion of intracellular Ca^{2+} by caffeine and ryanodine induces apoptosis of Chinese hamster ovary cells transfected with ryanodine receptor. *J. Biol. Chem.* 275:19978–19984.

Proenza, C., C. M. Wilkens, and K. G. Beam. 2000. Excitation-contraction coupling is not affected by scrambled sequence in residues 681–690 of the dihydropyridine receptor II-III loop. *J. Biol. Chem.* 275: 29935–29937.

Ríos, E., and G. Pizarro. 1991. Voltage sensor of excitation-contraction coupling in skeletal muscle. *Physiol. Rev.* 71:849–908.

Rossi, R., R. Bottinelli, V. Sorrentino, and C. Reggiani. 2001. Response to caffeine and ryanodine receptor isoforms in mouse skeletal muscles. *Am. J. Physiol. Cell Physiol.* 281:C585—C594.

Shirokova, N., J. García, and E. Ríos. 1998. Local calcium release in mammalian skeletal muscle. *J. Physiol.* 512.2:377–384.

Shirokova, N., R. Shirokov, D. Rossi, A. González, W. G. Kirsch, J. García, V. Sorrentino, and E. Ríos. 1999. Spatially segregated control of Ca^{2+} release in developing skeletal muscle of mice. *J. Physiol.* 521:483–495.

Shtifman, A., C. W. Ward, J. Wang, H. H. Valdivia, and M. F. Schneider. 2000. Effects of imperatoxin A on local sarcoplasmic reticulum Ca^{2+} release in frog skeletal muscle. *Biophys. J.* 79:814–827.

Schuhmeier, R. P., and W. Melzer. 2001. Determination of the rate of intracellular calcium release in myotubes. *Biophys. J.* 80:378A.

Sorrentino, V., V. Barone, and D. Rossi. 2000. Intracellular Ca^{2+} release channels in evolution. *Curr. Opin. Genet. Dev.* 10:662–667.

Sorrentino, V., and C. Reggiani. 1999. Expression of the ryanodine receptor type 3 in skeletal muscle. A new partner in excitation-contraction coupling? *Trends Cardiovasc. Med.* 9:54–61.

Sutko, J. L., and J. A. Airey. 1996. Ryanodine receptor Ca^{2+} release channels: does diversity in form equal diversity in function? *Physiol. Rev.* 76:1027–1071.

Takeshima, H., M. Iino, H. Takekura, M. Nishi, J. Kuno, O. Minowa, H. Takano, and T. Noda. 1994. Excitation-contraction uncoupling and muscular degeneration in mice lacking functional skeletal muscle ryanodine-receptor gene. *Nature.* 369:556–559.

Tanabe, T., K. G. Beam, B. A. Adams, T. Niidome, and S. Numa. 1990. Regions of the skeletal muscle dihydropyridine receptor critical for excitation-contraction coupling. *Nature.* 346:567–569.

Tripathy, A., W. Resch, L. Xu, H. H. Valdivia, and G. Meissner. 1998. Imperatoxin A induces subconductance states in Ca^{2+} release channels (ryanodine receptors) of cardiac and skeletal muscle. *J. Gen. Physiol.* 111:679–690.

Wilkens, C. M., N. Kasielke, B. E. Flucher, K. G. Beam, and M. Grabner. 2001. Excitation-contraction coupling is unaffected by drastic alteration of the sequence surrounding residues L720–L764 of the α1S II-III loop. *Proc. Natl. Acad. Sci. U.S.A.* 98:5892–5897.

Xu, X., M. B. Bhat, M. Nishi, H. Takeshima, and J. Ma. 2000. Molecular cloning of cDNA encoding a *Drosophila* ryanodine receptor and functional studies of the carboxyl-terminal calcium release channel. *Biophys. J.* 78:1270–1281.

Zhu, X., G. Gurrola, M. T. Jiang, J. W. Walker, and H. H. Valdivia. 1999. Conversion of an inactive cardiac dihydropyridine receptor II-III loop segment into forms that activate skeletal ryanodine receptors. *FEBS Lett.* 450:221–226.